Scientific Research Publishing

International Journal of Organic Chemistry, 2025, 15(2), 7-19
https://www.scirp.org/journal/ijoc
ISSN Online: 2161-4695
ISSN Print: 2161-4687

Synthesis and Characterization of Conjugated TPA-Based Azines Containing an Anthracene Moiety

Mamadou Lo*, Ablaye Diédhiou, Ibrahima Paka Manga, Bineta Sene, Abdoulaye Gassama

Laboratoire de Chimie et physique des Matériaux, Université Assane Seck de Ziguinchor, Ziguinchor, Sénégal
Email: *mlo@univ-zig.sn

How to cite this paper: Lo, M., Diédhiou, A., Manga, I.P., Sene, B. and Gassama, A. (2025) Synthesis and Characterization of Conjugated TPA-Based Azines Containing an Anthracene Moiety. *International Journal of Organic Chemistry*, **15**, 7-19.
https://doi.org/10.4236/ijoc.2025.152002

Received: April 1, 2025
Accepted: June 27, 2025
Published: June 30, 2025

Abstract

Azines are a class of compounds with significant potential in materials science due to their good electronic and optical properties. In this study, a series of three novel compounds incorporating one, two, and three azine-type bonds was synthesized via an acetic acid-catalyzed condensation reaction between 9-anthraldehyde hydrazone (AN-2) and formylated derivatives of triphenylamine (TPA): 4-(diphenylamino) benzaldehyde (TPA-1), 4,4''-(phenylazinediyl) dibenzaldehyde (TPA-2), and 4,4',4''-nitrilotribenzaldehyde (TPA-3). The chemical structures of the resulting azines (AZ-1, AZ-2, and AZ-3) were confirmed by nuclear magnetic resonance (NMR), infrared (IR), and mass spectrometry (MS). Their thermal properties were further investigated using thermogravimetric analysis (TGA) and differential scanning calorimetry (DSC), while their electronic properties were examined via Ultraviolet–visible (UV–visible) spectroscopy. The results indicate that the three azines exhibit distinct thermal behaviors while demonstrating good thermal stability. Furthermore, the azine linkage between the TPA and anthracene moieties has minimal influence on the electronic properties of the compounds, suggesting a limited conjugation effect across the azine bridge. This finding provides valuable insights for the design of azine-based functional materials for future applications.

Keywords

Anthracene, Triphenylamine, Azine, Spectroscopic Analysis, Thermal Characterization

1. Introduction

The synthesis of polyconjugated compounds is a rapidly growing and highly

promising field of research driven by their diverse applications, particularly in organic materials [1]-[9]. This synthesis typically involves the formation of one or more bonds that establish a connection between chromophores of the same or different nature [10] [11]. The linkages between chromophores are most commonly carbon-carbon (ethylenic or acetylenic) [12] or carbon-nitrogen bonds (azomethine or azine) [13]. Among polyconjugated compounds featuring a carbon–nitrogen bond, azine-based polyconjugated compounds (>C=N–N=C<) [14] remain significantly less explored than their azomethine counterparts (>C=N–) despite similar synthetic conditions [15]. Azines are organic compounds formed by the condensation of two aldehydes or ketones with hydrazine. They are classified into two categories, aldazines and ketazines, depending on whether the starting carbonyl compound is an aldehyde or a ketone [16]-[18]. Various strategies for the synthesis of symmetrical and unsymmetrical azines have been reported in literature [19]. Symmetrical azines can be readily synthesized, either directly or indirectly, by reacting hydrazine with excess aldehydes or ketones. However, synthesis of their unsymmetrical counterparts is challenging. Selective methods for the preparation of unsymmetrical azines have also been reported [20]. Azines exhibit a wide range of interesting chemical properties, making them valuable intermediates in organic syntheses. For example, they serve as key synthons for the construction of heterocycles [21], such as pyrazoles, purines, and pyrimidines [22]. Azines are also used to protect the carbonyl functional groups [23]. In this context, we focused on the synthesis of polyconjugated compounds that incorporate at least one azine bond. To this end, we synthesized a series of azine-based polyconjugated materials via condensation of triphenylamine (TPA) derivatives with a hydrazone derived from anthraldehyde. The coupling of anthraldehyde, a fluorophore [24] [25], with three different TPA derivatives known for their remarkable redox properties [26]-[29], led to the formation of three novel polyconjugated compounds bearing one, two, or three azine bonds. The electronic and thermal properties of the newly synthesized materials were investigated.

2. Results and Discussion

2.1. Synthesis of Azines

Three novel azines were synthesized via the acid-catalyzed condensation of hydrazone AN-2 with a series of three aldehydes derived from TPA. The syntheses of these azines are shown in **Scheme 1**. First, the key synthon AN-2 was prepared from anthraldehyde (AN-1) following a previously reported procedure [30]. Specifically, the condensation of commercially available anthracene-9-carbaldehyde (AN-1) with 65% hydrazine monohydrate in absolute ethanol in the presence of a catalytic amount of glacial acetic acid yielded hydrazone (AN-2) in 79% yield. Three formylated TPA derivatives, 4-(diphenylamino) benzaldehyde (TPA-1), 4,4'-(phenylazinediyl) dibenzaldehyde (TPA-2), and 4,4',4''-nitrilobenzaldehyde (TPA-3), were synthesized from TPA via the Vilsmeier–Haack reaction, following a previously reported method [28] [31]. The target compounds AZ-1, AZ-2, and

AZ-3, which incorporated one, two, and three azine bonds, respectively, were obtained by condensing the amine functionality of AN-2 with the formyl derivatives of TPA (TPA-1, TPA-2, and TPA-3). The reactions were performed under stoichiometric conditions in the presence of a catalytic amount of glacial acetic acid. After recrystallization from absolute ethanol, the final compounds were obtained as powders: yellow for AZ-1 and orange for both AZ-2 and AZ-3 with yields of 35%, 92%, and 75%, respectively.

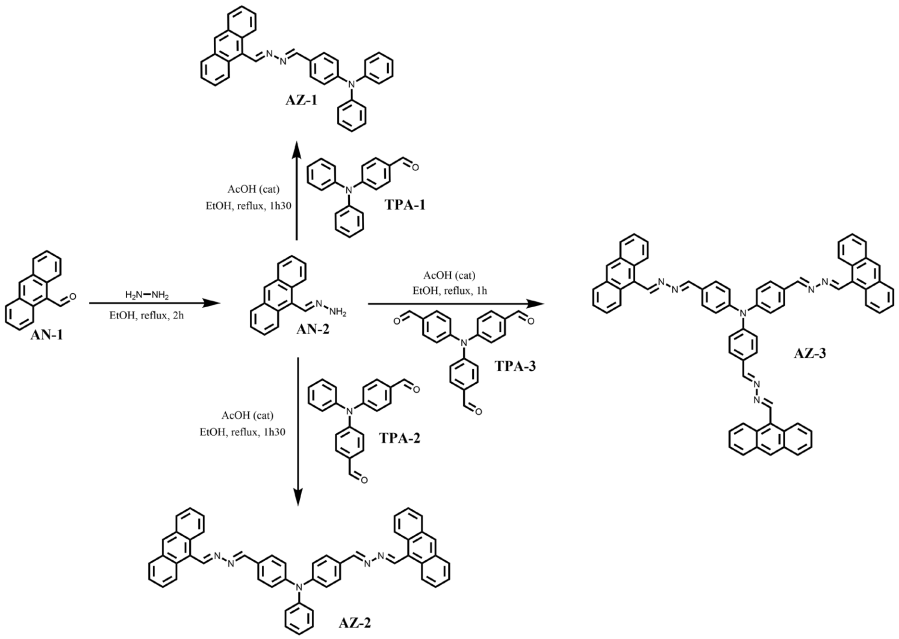

Scheme 1. Overall reaction in the synthesis of azines.

2.2. Structural Characterization of Azines

In the proton NMR spectrum of hydrazone AN-2, the formation of the imine functional group is evidenced by the presence of singlets at 8.80 and 5.91 ppm, corresponding to the imine proton and the two protons attached to the nitrogen atom, respectively. The remaining signals corresponded to the aromatic protons of the anthracene core. In the carbon NMR spectrum of AN-2, the carbon bearing the imine function resonates at 140.94 ppm and was the most unshielded carbon. These results are consistent with the IR spectrum, which exhibited a band at 3363 cm^{-1} corresponding to the NH_2 group and a band at 1620.80 cm^{-1} associated with the CH=N imine function, confirming the formation of compound AN-2. The formation of the azine moiety and assignment of protons in compounds AZ-1 and AZ-2 can be demonstrated by overlaying the proton NMR spectra of AN-2 with those of the corresponding formylated TPA derivatives (Figure 1 and Figure 2).

The proton NMR spectra of compounds AZ-1 and AZ-2 revealed the disappearance of the two protons attached to the nitrogen atom of hydrazone AN-2 as well as the aldehyde proton of the TPA derivative. This disappearance is accompanied by the appearance of a new imine proton, resonating at 9.93 ppm for AZ-

1 and 9.90 ppm for AZ-2. This proton, the most unshielded proton in each spectrum, reflects the strong conjugation effect induced by the TPA moiety, confirming the formation of azine bonds in AZ-1 and AZ-2. Additionally, the aromatic protons of the anthracene core (highlighted with a solid line frame) and those of the TPA unit (highlighted with a dashed line frame) remain well distinguishable. The formation of the azine functional group is further supported by the carbon NMR spectra, which exhibit characteristic peaks at 162.22 and 160.97 ppm for AZ-2 and at 162.57 and 160.49 ppm for AZ-1. In the IR spectra, the presence of two absorption bands at 1584.48 and 1484.24 cm^{-1} for AZ-1 and at 1589.06 and 1504.04 cm^{-1} for AZ-2 confirms the formation of the azine bond. Final confirmation of the formation of AZ-1 and AZ-2 was confirmed using mass spectrometry. The molecular ion peaks at m/z = 476.21 and m/z = 706.29, correspond to the protonated molecular ions $[(AZ\text{-}1) + H]^+$ and $[(AZ\text{-}2) + H]^+$, respectively. Unlike azines AZ-1 and AZ-2, azine AZ-3 has low solubility in conventional organic solvents, which prevents the acquisition of high-resolution NMR spectra. This limited solubility is likely due to strong π-stacking interactions between the aromatic rings in the solution. Consequently, the characterization of AZ-3 was primarily based on infrared spectroscopy and mass spectrometry. The IR spectrum of AZ-3 exhibits two strong absorption bands characteristic of the azine functional group at 1592.89 and 1503.19 cm^{-1}. Mass spectrometry confirmed the formation of AZ-3. The presence of peaks at m/z = 936.38 and m/z = 734.29, supports its molecular structure. The molecular ion peak at m/z = 936.38 corresponded to $[(AZ\text{-}3) + H]^+$, whereas the peak at m/z = 734.29 was attributed to a fragment resulting from the cleavage of one of the N–N bonds in AZ-3. Additionally, a comparison between the calculated and experimental isotopic profiles of $[(AZ\text{-}3) + H]^+$ further confirms the formation of AZ-3.

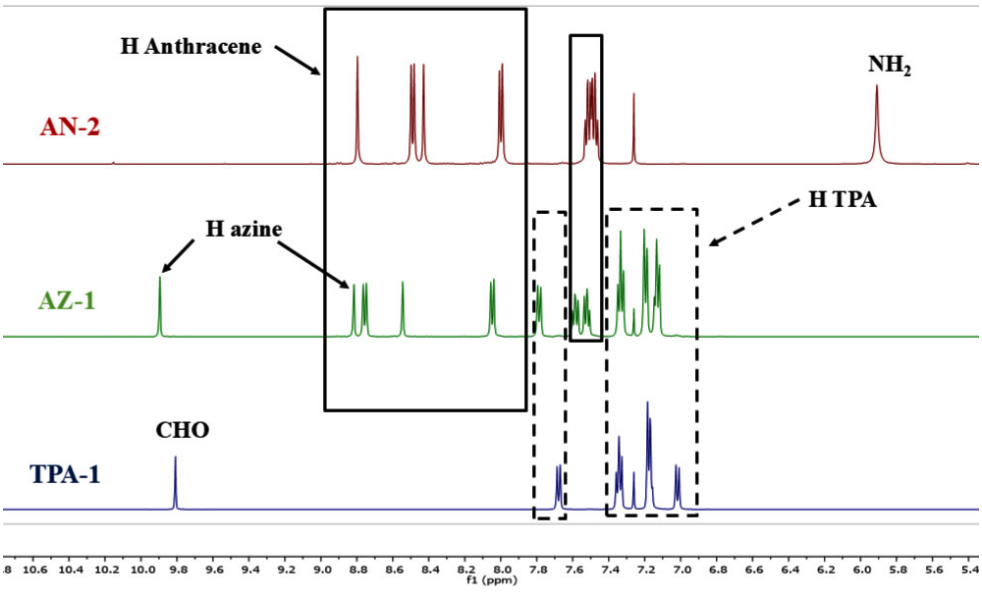

Figure 1. Overlay of the proton NMR spectra of AN-2, AZ-1, and TPA-1.

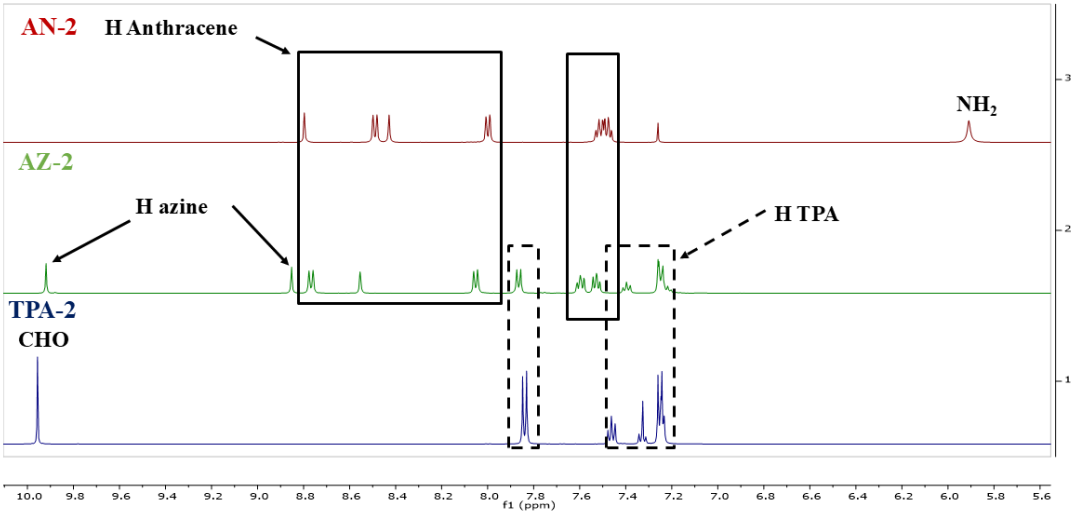

Figure 2. Overlay of the proton NMR spectra of AN-2, AZ-2, and TPA-2.

2.3. UV-Visible Characterization of Azines in Solution

The optical properties of azines AZ-1, AZ-2, and AZ-3 in chloroform solution were investigated via UV−visible spectroscopy. Similar to the proton NMR analysis, the spectra of AZ-1, AZ-2, and AZ-3 were compared to those of their precursor, hydrazone AN-2. The UV-visible spectra are presented in **Figure 3**.

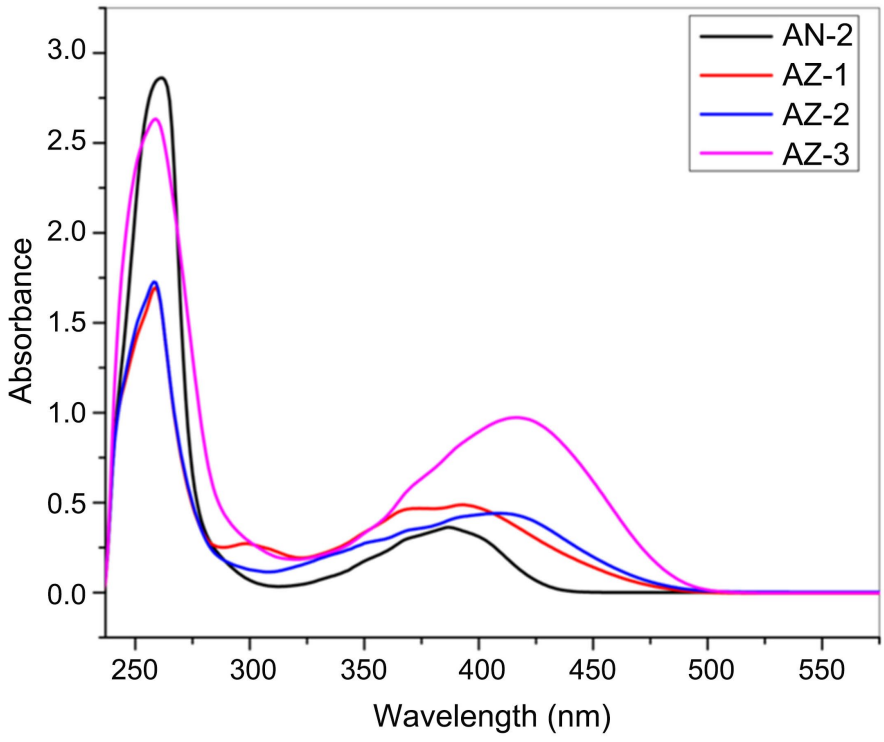

Figure 3. UV−visible spectra of AN-2, AZ-1, AZ-2, and AZ-3.

The key UV−visible data for the four compounds are summarized in **Table 1**.

Table 1. UV-Visible data of AN-2, AZ-1, AZ-2, and AZ-3.

Compounds	λ_1 (nm)	λ_2 (nm)
AN-2	260	387
AZ-1	258	392
AZ-2	258	410
AZ-3	258	416

Analysis of the UV-visible spectra revealed similar features for all four compounds in chloroform, with each spectrum displaying two main absorption bands. The first absorption band, with a maximum at λ_1 = 258 or 260 nm, was attributed to the π-π^* transition of the anthracene core [32]. The second maximum absorption band, with λ_2 values ranging between 387 and 416 nm, corresponds to the n–π^* transition of the imine group [33]. Two key observations can be made. First, the formation of the azine bond induces minimal perturbation of the electronic transitions originating from the anthracene moiety. Second, a slight redshift in λ_2 was observed with increasing number of imine groups in azines AZ-1, AZ-2, and AZ-3. These subtle changes in the UV-visible spectra confirm that the azine bond acts as a conjugation blocker between the anthracene and TPA moieties [34].

2.4. Study of the Thermal Properties of Azines

The thermal behavior of azines was investigated by thermogravimetric analysis (TGA), derivative thermogravimetry (DTG), and differential scanning calorimetry (DSC). TGA was performed on AZ-1, AZ-2, and AZ-3 to evaluate their thermal stability and decomposition behavior. The samples were heated to 600˚C under nitrogen atmosphere at a heating rate of 10˚C/min. **Figure 4** presents the TGA curves (top), which display the mass loss as a function of temperature, and DTG curves (bottom), which highlight the corresponding decomposition steps by showing the rate of mass loss.

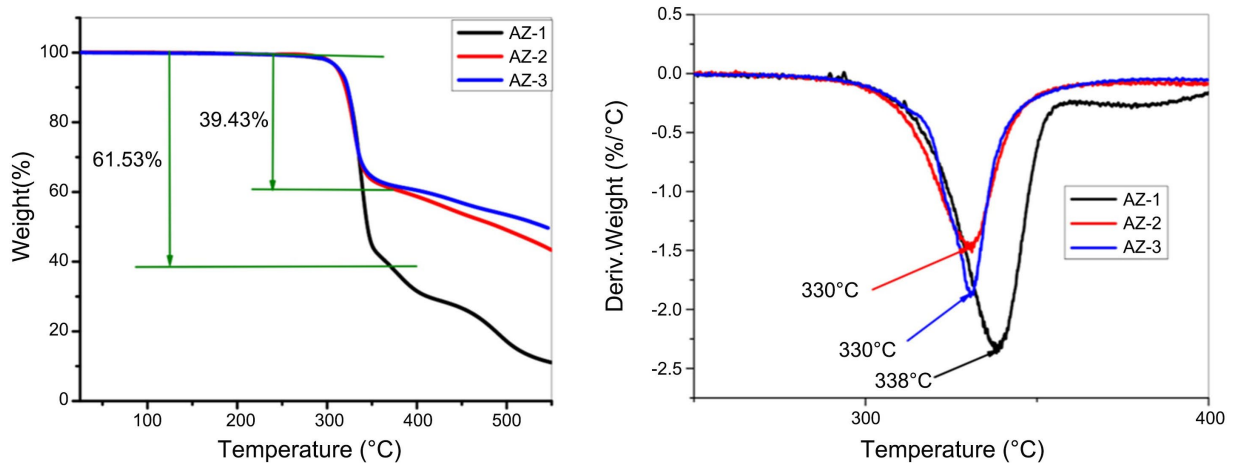

Figure 4. TGA curves (left) and DTG curves (right) for AZ-1, AZ-2, and AZ-3 azines.

Analysis of the TGA curves indicated that all three azines exhibited high thermal stability up to 300˚C with no detectable mass loss. This suggests that their molecular structures remain intact up to this temperature. Above 300˚C, significant thermal decomposition occurred for all three compounds, as evidenced by the substantial mass loss between 300˚C and 355˚C. The DTG curves reveal a maximum peak at 338˚C for AZ-1 and two peaks at 330˚C, corresponding to the decomposition temperatures of AZ-2 and AZ-3. The estimated mass loss at the decomposition temperature of the azines was 61.53% (calculated: 60%) for AZ-1 and 39.43% for the other two azines (calculated: 38.16% for AZ-2 and 39.02% for AZ-3). The molecular fragments corresponding to each mass-loss step are represented by dotted lines in **Figure 5** [35]. The small variation in the mass loss between the theoretical and experimental values suggests that the decomposition process of our compounds begins with a break at the azine bond. At 600˚C, the carbon residue rates of the three azines were 9% for AZ-1, 37% for AZ-2, and 45% for AZ-3. This variation is primarily attributed to the number of aromatic rings in the structures [36].

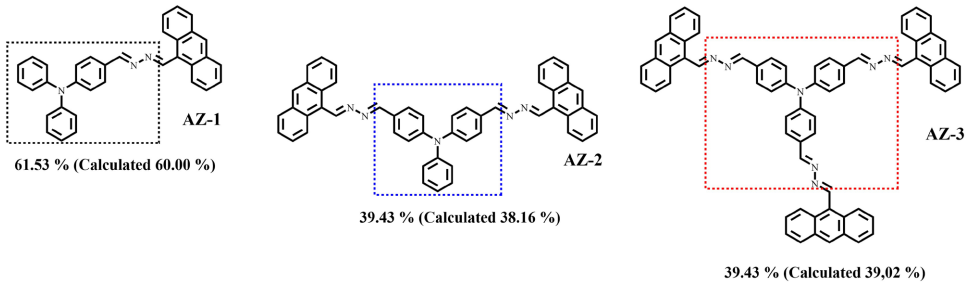

Figure 5. Decomposition profile of azines obtained from TGA analysis.

DSC measurements were conducted to analyze the thermal transitions of the azines. The first and second heating cycles were performed at a constant rate of 10˚C/min. The second heating cycle was performed immediately after rapid cooling. **Figure 6** shows the DSC thermograms from the first and second heating cycles for azines AZ-1 and AZ-2.

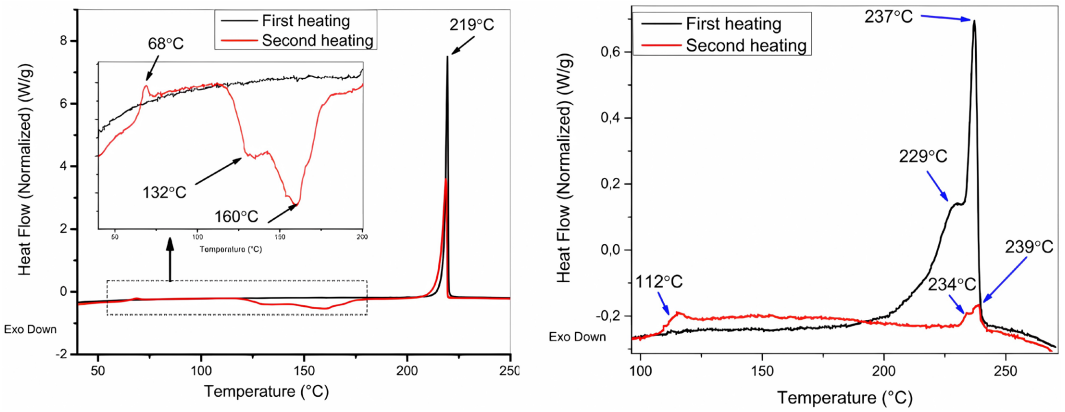

Figure 6. DSC thermograms of AZ-1 (left) and AZ-2 (right) azines.

Analysis of the DSC curves of AZ-1 and AZ-2 during the first heating cycle revealed three distinct endothermic peaks. These values correspond to the melting temperatures of azine AZ-1 at 219˚C and the melting temperatures of azine AZ-2 at 229˚C and 237˚C, respectively. During the second heating cycle, azine AZ-1 exhibited a glass transition (Tg) at 68˚C, followed by two exothermic cold crystallization events at 132˚C and 160˚C. In contrast, azine AZ-2 undergoes a glass transition at Tg = 112˚C, followed by two endothermic melting peaks at 234˚C and 239˚C. These results suggest that AZ-1 is semicrystalline whereas AZ-2 is amorphous [37]. Overall, DSC analysis confirmed that both AZ-1 and AZ-2 function as molecular glasses, primarily differing in their Tg values [38]. Notably, no thermal transitions were observed for azine AZ-3 during either the first or second heating cycle, as confirmed by DSC analysis.

3. Experimental

3.1. Materials and Methods Authors

Commercially available reagents and solvents (ACS grade) were used as purchased, without further purification. NMR spectra were recorded using a Bruker Advance 500 spectrometer (500 MHz). Chemical shifts are given in ppm and were determined using solvent as a reference. The abbreviations used to describe the NMR signals are as follows: s, singlet; d, doublet; m, multiplet. All coupling constants are in hertz. Mass spectrometry was performed on a Bruker Daltonics microTOF spectrometer (Bruker Daltonik GmbH, Bremen, Germany) by the Service de Spectrométrie de Masse de la Fédération de Chimie "Le Bel" (FR 2010). All the UV-visible measurements were performed in chloroform at room temperature. UV−visible spectra were obtained using a Cary 6000i UV-visible spectrophotometer. Infrared (IR) spectra were recorded on a PerkinElmer Spectrum IR spectrometer (Spectrum One, FT-IR Spectrometer) within the range of 800 - 4000 cm^{-1}. TGA and DSC were performed using an SDT Q600 (TA Instruments) and a DSC Q2000 (TA Instruments) by Laboratoire de Caractérisation des Matériaux Polymères (LCMP), Université de Montréal, Complexe des Sciences, Campus MIL, 1375 Avenue Thérèse-Lavoie Roux, Montréal, Québec, H2V 0B3.

3.2. Synthesis of the Compounds

3.2.1. Synthesis of the Formulated TPA

These three formylated TPAs (TPA-1, TPA-2, and TPA-3) were synthesized from TPA according to previously described procedures [28].

3.2.2. Synthesis of 9-Anthraldehyde Hydrazone (AN-2)

To a solution of 9-anthraldehyde (1.06 g, 5.16 mmol) in 10 ml of absolute ethanol at room temperature was added 64% - 65% hydrazine monohydrate (3 ml, 618,4 mmol). The reaction mixture was then heated under reflux for 2 h. After cooling to room temperature and filtering, a yellow powder was obtained, which was recrystallized from ethanol to provide AN-2 as a yellow solid. Yield: 0.90 g (79%). RMN ^{1}H (500 MHz, $CDCl_3$) δ ppm: 8.80 (s, 1H), 8.49 (d, J = 8.7 Hz, 2H), 8.43 (s,

1H), 8.00 (d, J = 8.1 Hz, 2H), 7.55–7.44 (m, 4H), 5.91 (s, 2H). RMN ^{13}C (126 MHz, $CDCl_3$) δ ppm: 140.94, 131.42, 129.96, 128.84, 128.30, 126.73, 126.28, 125.53, 125.22, 125.16, 77.34, 77.29, 77.08, 76.83. FTIR-ATR (cm^{-1}): 3363 (NH_2), 1620, 80 (CH=N).

3.2.3. Synthesis of Compound AZ-1

A suspension of 9-anthraldehyde hydrazone (111 mg, 1.1 mmol) and TPA-1 (1.25 g, 1.2 mmol) in 10 ml of absolute ethanol was stirred and slightly warmed until dissolution of the solid, after which 1 to 2 drops of glacial acetic acid were added. The reaction mixture was then heated under reflux and stirred for 2 h. After cooling to room temperature and filtering, an orange powder was obtained, which was washed with cold ethanol and dried. Yield: 191 mg (35%). RMN ^{1}H (500 MHz, $CDCl_3$) δ ppm: 9.93 (s, 1H), 8.85 (s, 1H), 8.79 (d, J = 8.8 Hz, 2H), 8.58 (s, 1H), 8.08 (d, J = 8.3 Hz, 2H), 7.82 (d, J = 8.6, 1.7 Hz, 2H), 7.62 (m, 2H), 7.56 (m, 2H), 7.37 (m, 4H), 7.26 - 7.20 (m, 4H), 7.20 - 7.14 (m, 4H). RMN ^{13}C (126 MHz, $CDCl_3$) δ ppm: 162.56, 160.54, 150.86, 146.94, 131.41, 130.68, 130.38, 129.91, 129.58, 129.02, 127.06, 126.91, 125.65, 125.59, 125.44, 125.35, 124.18, 121.54, 77.34, 77.08, 76.83. MS (ESI^+): m/z calculated for $C_{34}H_{26}N_3^+$ = 476.21 $[M + H]^+$; found: 476.21. FTIR-ATR (cm^{-1}): 1584.88 and 1484.84 (CH=N).

3.2.4. Synthesis of Compound AZ-2

The synthesis was analogous to that used for the synthesis of AZ-1 with 9-anthraldehyde hydrazone (220 mg, 1 mmol) and TPA-2 (150 mg, 0.5 mmol). Compound AZ-2 was obtained as an orange-colored solid. Yield: 321 mg (92%). RMN ^{1}H (500 MHz, $CDCl_3$) δ ppm: 9.90 (s, 1H), 8.83 (s, 1H), 8.75 (d, J = 8.9 Hz, 2H), 8.53 (s, 1H), 8.03 (d, J = 8.4 Hz, 2H), 7.84 (d, J = 8.6 Hz, 2H), 7.58 (m, 2H), 7.51 (m, 2H), 7.41 - 7.34 (m, 1H), 7.25 - 7.17 (m, 4H). RMN ^{13}C (126 MHz, $CDCl_3$) δ ppm: 162.18, 160.93, 149.88, 146.33, 131.35, 130.66, 130.49, 129.97, 129.80, 129.00, 128.45, 127.08, 126.72, 126.25, 125.42, 125.41, 125.24, 125.04, 124.56, 123.37, 121.35, 77.28, 77.02, 76.77. MS (ESI^+): m/z calculated for $C_{51}H_{36}N_5^+$ = 706.3 $[M + H]^+$; found: 706.29. FTIR-ATR (cm^{-1}): 1589.06 and 1504.04 (CH=N).

3.2.5. Synthesis of Compound AZ-3

The synthesis was analogous to that used for the synthesis of AZ-1 with 9-anthraldehyde hydrazone (220 mg, 1 mmol) and TPA-3 (98.5 mg, 0.3 mmol). Compound AZ-2 was obtained as an orange-colored solid. Yield: 208 mg (75%). MS (ESI^+): m/z calculated for $C_{66}H_{46}N_7^+$ = 936.38 $[M + H]^+$; found 936.38. FTIR-ATR (cm^{-1}): 1592.85 and 1503.19 (CH=N).

4. Conclusion

In this study, we successfully synthesized three novel azines (AZ-1, AZ-2, and AZ-3) via the acid-catalyzed condensation of their hydrazone precursors and formylated triphenylamine derivatives. Azines were obtained in satisfactory yields and their structures were confirmed by NMR, IR, and MS. Complete proton assignments for AZ-1 and AZ-2 were achieved via a combination of 1D (^{1}H, ^{13}C,

and DEPT-135) and 2D (COSY and HSQC) NMR techniques. UV-visible characterization in chloroform revealed that the azine bridge had minimal influence on the electronic communication between the anthracene and TPA moieties. Thermal analysis further demonstrated that while the three azines exhibited distinct thermal behaviors, they had good thermal stability, with decomposition temperatures exceeding 300˚C. These findings suggest that azine-based materials can offer a balance between structural tunability and robustness, making them promising candidates for further functionalization in materials science applications. Additional UV-visible studies in solution are planned to deepen our understanding of these materials, particularly those in which a wider range of polar and nonpolar solvents are used to assess their solvatochromic properties. Furthermore, solid-state UV-visible investigations, along with a comprehensive photophysical study, will provide deeper insight into their optical behavior. Finally, an electrochemical study of the redox properties was conducted to evaluate their potential for electronic and optoelectronic applications.

Acknowledgements

The authors would like to thank the CLAC laboratory of the University of Strasbourg for performing the characterizations (NMR and MS), and Professor Gary Hanan's group at the University of Montreal for thermal measurements (TGA and DSC) and additional characterizations (IR and UV−Vis).

Conflicts of Interest

The authors declare no conflicts of interest regarding the publication of this paper.

References

[1] Beverina, L., Sassi, M., Mattiello, S. and Fappani, A. (2023) Polyconjugated Materials for Printed (Opto)electronics: Introducing Sustainability. *Synlett*, **35**, 1629-1647. https://doi.org/10.1055/a-2191-6011

[2] Verbitskiy, E.V., Rusinov, G.L., Chupakhin, O.N. and Charushin, V.N. (2021) Azines as Unconventional Anchoring Groups for Dye-Sensitized Solar Cells: The First Decade of Research Advances and a Future Outlook. *Dyes and Pigments*, **194**, Article ID: 109650. https://doi.org/10.1016/j.dyepig.2021.109650

[3] Acker, P., Speer, M.E., Wössner, J.S. and Esser, B. (2020) Azine-Based Polymers with a Two-Electron Redox Process as Cathode Materials for Organic Batteries. *Journal of Materials Chemistry A*, **8**, 11195-11201. https://doi.org/10.1039/d0ta04083e

[4] Zhou, Z., Sun, H., Qi, Q. and Zhao, X. (2024) Converting Azine Linkage into Highly Stable (Thio)urea-Based Bicyclic-Fused-Ring Connections in Covalent Organic Frameworks via Criss-Cross [3+2] Cycloaddition. *CCS Chemistry*, **6**, 2230-2240. https://doi.org/10.31635/ccschem.023.202303568

[5] Kagatikar, S., Acharya, S., MP, Y., Sunil, D., Kekuda, D., Abdul Salam, A.A., *et al.* (2023) Orthovanillin Azine Ester as a Potential Functional Material for Organic Electronic Devices. *Journal of Molecular Structure*, **1289**, Article ID: 135781. https://doi.org/10.1016/j.molstruc.2023.135781

[6] Takagi, S.I., Hayakawa, M. and Fukazawa, A. (2023) Stereoselective Synthesis and

Characterization of Indenone Azine-Based Electron-Accepting π-Conjugated Systems. *Chemistry—A European Journal*, **29**, e202300181. https://doi.org/10.1002/chem.202300181

[7] Sobarzo, P.A., Jessop, I.A., Pérez, Y., Hauyon, R.A., Velázquez-Tundidor, M.V., Medina, J., *et al.* (2022) Synthesis of Dimethyl- and Diphenylsilane-Based Oligo(azine)s: Thermal, Optical, Electronic, and Morphological Properties. *Journal of Applied Polymer Science*, **139**, e52911. https://doi.org/10.1002/app.52911

[8] Poojary, S., Sunil, D., Kekuda, D. and Sreenivasa, S. (2018) Fluorescent Aromatic Symmetrical Azines: Synthesis and Appraisal of Their Photophysical and Electrochemical Properties. *Optical Materials*, **85**, 1-7. https://doi.org/10.1016/j.optmat.2018.08.020

[9] Dalapati, S., Jin, S., Gao, J., Xu, Y., Nagai, A. and Jiang, D. (2013) An Azine-Linked Covalent Organic Framework. *Journal of the American Chemical Society*, **135**, 17310-17313. https://doi.org/10.1021/ja4103293

[10] Madhu, M., Ramakrishnan, R., Vijay, V. and Hariharan, M. (2021) Free Charge Carriers in Homo-Sorted Π-Stacks of Donor-Acceptor Conjugates. *Chemical Reviews*, **121**, 8234-8284. https://doi.org/10.1021/acs.chemrev.1c00078

[11] Wang, C., Du, T., Liang, Z., Zhu, J., Ren, J. and Deng, Y. (2021) Synthesis of Low-Bandgap Small Molecules by Extending the π-Conjugation of the Termini in Quinoidal Compounds. *Journal of Materials Chemistry C*, **9**, 2054-2062. https://doi.org/10.1039/d0tc04962j

[12] Yao, D., Shi, L., Sun, Z., Blanchard-Desce, M., Mongin, O., Paul, F., *et al.* (2021) New Fluorescent Tetraphenylporphyrin-Based Dendrimers with Alkene-Linked Fluorenyl Antennae Designed for Oxygen Sensitization. *Comptes Rendus. Chimie*, **24**, 57-70. https://doi.org/10.5802/crchim.99

[13] Bishop, S., Tremblay, M., Gellé, A. and Skene, W.G. (2019) Understanding Color Tuning and Reversible Oxidation of Conjugated Azomethines. *The Journal of Physical Chemistry A*, **123**, 2687-2693. https://doi.org/10.1021/acs.jpca.8b10593

[14] Chourasiya, S.S., Kathuria, D., Wani, A.A. and Bharatam, P.V. (2019) Azines: Synthesis, Structure, Electronic Structure and Their Applications. *Organic & Biomolecular Chemistry*, **17**, 8486-8521. https://doi.org/10.1039/c9ob01272a

[15] Petrus, M.L., Bouwer, R.K.M., Lafont, U., Murthy, D.H.K., Kist, R.J.P., Böhm, M.L., *et al.* (2013) Conjugated Poly(azomethine)s via Simple One-Step Polycondensation Chemistry: Synthesis, Thermal and Optoelectronic Properties. *Polymer Chemistry*, **4**, 4182-4191. https://doi.org/10.1039/c3py00433c

[16] Alkorta, I., Blanco, F. and Elguero, J. (2007) Computational Studies of the Structure of Aldazines and Ketazines. Part 1. Simple Compounds. *Arkivoc*, **2008**, 48-56. https://doi.org/10.3998/ark.5550190.0009.706

[17] Barluenga, J., Fustero, S., Gómez, N. and Gotor, V. (2002) A New Method for the Synthesis of Unsymmetric Azines: Alkylidene Group Exchange between Azines and Lmines. *Synthesis*, **1982**, 966-967. https://doi.org/10.1055/s-1982-30024

[18] Rosini, G., Soverini, M. and Ballini, R. (1983) Azines from *erythro*-1,2-Diaryl-2-(2-Tosylhydrazino)-Ethan-1-Ol Derivatives by Acid Treatment. *Synthesis*, **1983**, 909-910. https://doi.org/10.1055/s-1983-30562

[19] Safari, J. and Gandomi-Ravandi, S. (2014) Structure, Synthesis and Application of Azines: A Historical Perspective. *RSC Adv.*, **4**, 46224-46249. https://doi.org/10.1039/c4ra04870a

[20] Bodtke, A., Pfeiffer, W., Ahrens, N. and Langer, P. (2005) Horseradish Peroxidase (HRP) Catalyzed Oxidative Coupling Reactions Using Aqueous Hydrogen Peroxide:

An Environmentally Benign Procedure for the Synthesis of Azine Pigments. *Tetrahedron*, **61**, 10926-10929. https://doi.org/10.1016/j.tet.2005.08.103

[21] Safari, J., Gandomi-Ravandi, S. and Ghotbinejad, M. (2016) Ultrasound-Promoted Synthesis of Novel Fused Heterocycles by Criss-Cross Cycloaddition. *Journal of Saudi Chemical Society*, **20**, 20-23. https://doi.org/10.1016/j.jscs.2012.02.009

[22] Galeta, J., Man, S. and Potáček, M. (2009) Non-Symmetrical Allenyl Azines and Their Transformations Leading to New Heterocyclic Skeletons. *Arkivoc*, **2009**, 245-259. https://doi.org/10.3998/ark.5550190.0010.625

[23] Nanjundaswamy, H.M. and Pasha, M.A. (2006) Selective Protection of Carbonyl Compounds as Azines and Their Facile Regeneration. *Synthetic Communications*, **36**, 3161-3165. https://doi.org/10.1080/00397910600908835

[24] Kathiravan, A. and Narayanan, M. (2025) Anthraldehyde-Based Aggregation Induced Emissive Probe for Hydroxylamine Detection and Latent Fingerprint Imaging. *Microchemical Journal*, **208**, 112573. https://doi.org/10.1016/j.microc.2024.112573

[25] Huang, D., Gao, Z., Yi, H., Bing, Y., Niu, C., Guo, Q., *et al.* (2015) A Facile Fluorescent Probe Based on Anthraldehyde for Trace Fe(III) Ion Determination in Neutral Aqueous Solution. *Analytical Methods*, **7**, 353-358. https://doi.org/10.1039/c4ay02211d

[26] Rybakiewicz, R., Zagorska, M. and Pron, A. (2016) Triphenylamine-Based Electroactive Compounds: Synthesis, Properties and Application to Organic Electronics. *Chemical Papers*, **71**, 243-268. https://doi.org/10.1007/s11696-016-0097-0

[27] Agarwala, P. and Kabra, D. (2017) A Review on Triphenylamine (TPA) Based Organic Hole Transport Materials (HTMs) for Dye Sensitized Solar Cells (DSSCs) and Perovskite Solar Cells (PSCs): Evolution and Molecular Engineering. *Journal of Materials Chemistry A*, **5**, 1348-1373. https://doi.org/10.1039/c6ta08449d

[28] Li, C., Yang, W., Zhou, W., Zhang, M., Xue, R., Li, M., *et al.* (2016) Branching Effect for Aggregation-Induced Emission in Fluorophores Containing Imine and Triphenylamine Structures. *New Journal of Chemistry*, **40**, 8837-8845. https://doi.org/10.1039/c6nj01558a

[29] Sun, N., Su, K., Zhou, Z., Tian, X., Jianhua, Z., Chao, D., *et al.* (2019) High-Performance Emission/Color Dual-Switchable Polymer-Bearing Pendant Tetraphenylethylene (TPE) and Triphenylamine (TPA) Moieties. *Macromolecules*, **52**, 5131-5139. https://doi.org/10.1021/acs.macromol.9b00079

[30] Kaur, N. and Kaur, B. (2020) Colorimetric and Fluorescent Multi-Ion Recognition by Anthracene Appended Di-Schiff Base Chemosensor. *Inorganic Chemistry Communications*, **121**, Article ID: 108239. https://doi.org/10.1016/j.inoche.2020.108239

[31] Mongin, O., Mallegol, T., Gmouh, S., Meziane, M.A. and Blanchard-Desce, M. (2005) Practical and Efficient Synthesis of Tris(4-Formylphenyl)amine, a Key Building Block in Materials Chemistry. *Synthesis*, **2005**, 1771-1774. https://doi.org/10.1055/s-2005-865336

[32] Andiappan, K., Sanmugam, A., Deivanayagam, E., Karuppasamy, K., Kim, H. and Vikraman, D. (2018) *In Vitro* Cytotoxicity Activity of Novel Schiff Base Ligand-Lanthanide Complexes. *Scientific Reports*, **8**, Article No. 3054. https://doi.org/10.1038/s41598-018-21366-1

[33] Kaur, B., Gupta, A. and Kaur, N. (2020) A Simple Schiff Base as a Multi Responsive and Sequential Sensor Towards Al^{3+}, F^{-} and Cu^{2+} Ions. *Journal of Photochemistry and Photobiology A*: *Chemistry*, **389**, Article ID: 112140. https://doi.org/10.1016/j.jphotochem.2019.112140

[34] Lewis, M. and Glaser, R. (2002) The Azine Bridge as a Conjugation Stopper: An NMR Spectroscopic Study of Electron Delocalization in Acetophenone Azines. *The Journal*

of Organic Chemistry, **67**, 1441-1447. https://doi.org/10.1021/jo011117o

[35] Wang, L., Guo, D., Wang, Y. and Zheng, C. (2014) 4-Hydroxy-3-methoxy-benzaldehyde Series Aroyl Hydrazones: Synthesis, Thermostability and Antimicrobial Activities. *RSC Advances*, **4**, 58895-58901. https://doi.org/10.1039/c4ra11747f

[36] Yan, K., Chen, H., Zhu, C., Ke, Z., Li, D., Wang, M., *et al.* (2023) Synthesis and Characterization of Novel Triphenylamine—Containing Electrochromic Polyimides with Benzimidazole Substituents. *Molecules*, **28**, Article No. 2029. https://doi.org/10.3390/molecules28052029

[37] Kumar, S. and Patil, S. (2015) High T_g Fluoranthene-Based Electron Transport Materials for Organic Light-Emitting Diodes. *New Journal of Chemistry*, **39**, 6351-6357. https://doi.org/10.1039/c5nj00750j

[38] Bijak, K., Sek, D., Siwy, M., Grucela-Zajac, M., Janeczek, H., Wiacek, M., *et al.* (2014) Spectral, Electrochemical and Thermal Characteristics of Glass Forming Hydrazine Derivatives. *Optical Materials*, **37**, 498-510. https://doi.org/10.1016/j.optmat.2014.07.013